LANGMUIR Article
Cite This: Langmuir 2018, 34, 6777−6783
pubs.acs.org/Langmuir

Redefining Molecular Amphipathicity in Reversing the "Coffee-Ring Effect": Implications for Single Base Mutation Detection

Chi Huang,[†,∥] Jie Wang,[‡,∥] Xiaobo Lv,[‡] Liu Liu,[§] Ling Liang,[†] Wei Hu,[§] Changliang Luo,[§] Fubing Wang,[§] and Quan Yuan*[,†]

[†]Institute of Chemical Biology and Nanomedicine, Molecular Science and Biomedicine Laboratory, State Key Laboratory of Chemo/Biosensing and Chemometrics, College of Chemistry and Chemical Engineering, Hunan University, Changsha 410082, China

[‡]Key Laboratory of Analytical Chemistry for Biology and Medicine (Ministry of Education), College of Chemistry and Molecular Sciences and [§]Department of Laboratory Medicine & Center for Gene Diagnosis, Zhongnan Hospital, Wuhan University, Wuhan 430072, China

Supporting Information

ABSTRACT: The "coffee ring effect" is a natural phenomenon wherein sessile drops leave ring-shaped structures on the solid surfaces upon drying. It drives a nonuniform deposition of suspended compounds on the substrates, which adversely affects many processes, including surface-assisted biosensing and molecular self-assembly. In this study, we describe how the coffee ring effect can be eliminated by controlling the amphipathicity of the suspended compounds, for example, DNA modified with hydrophobic dye. Specifically, nuclease digestion of the hydrophilic DNA end converts the dye-labeled molecule into an amphipathic molecule (one with comparably weighted hydrophobic and hydrophilic ends) and reverses the coffee ring effect and results in a uniform disk-shaped feature deposition of the dye. The amphipathic product decreases the surface tension of the sessile drops and induces the Marangoni flow, which drives the uniform distribution of the amphipathic dye-labeled product in the drops. As a proof of concept, this strategy was used in a novel enzymatic amplification method for biosensing to eliminate the coffee ring effect on a nitrocellulose membrane and increase assay reliability and sensitivity. Importantly, the reported strategy for eliminating the coffee ring effect can be extended to other sessile drop systems for potentially improving assay reliability and sensitivity.

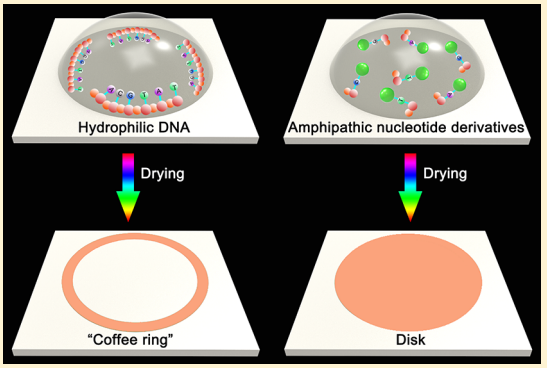

INTRODUCTION

The coffee ring effect refers to the often observed natural phenomenon that sessile drops containing dissolved or suspended compounds leave ringlike structures on the solid surfaces upon drying.[1−5] Previous studies suggest that the outward capillary flow caused by nonuniform evaporation of solvent carries the suspended compounds to the periphery of sessile drops during evaporation, leading to the form a "coffee ring" upon drying.[1,6−10] The coffee ring effect causes the nonuniform deposition of suspended compounds on the underlying surface, and it adversely impacts many processes involving surface-assisted biosensing, inkjet printing, molecular self-assembly, and painting.[11−17] For instance, in surface-based biosensing, where an aliquot of sensing solution is dried on a substrate, the nonuniform deposition of biosensing probes can lead to significant variations in signal intensity across the test zone, which decreases assay uniformity, reliability, and sensitivity.[18−22] Previous studies suggest that the formation of coffee ring is correlated with the charge,[23] amphipathicity,[24] and shape[2] of the suspended compounds,[3] thus chemical molecules with highly programmable physicochemical properties hold good promise to reverse the coffee ring effect.

DNA molecules provide great versatility to redefine their physicochemical properties in a user-defined manner through chemical modification.[25−29] Many sites on DNA molecules, such as the 5′-/3′-termini, the 2′-/4′-positions of the ribose and the bases, can be modified with functional moieties.[30−34] Researchers showed that the properties of DNA molecules such as amphipathicity and average charge density can be easily tuned by chemical modification.[28,35] For instance, researchers have designed amphipathic DNA by covalent linking of a lipid molecule on the termini.[36] The DNA molecules with highly programmable physicochemical properties can serve as the ideal molecules to reverse the coffee ring effect in sessile drop systems.

Herein, we reported that the nuclease digestion of hydrophobic molecules labeled DNA to generate amphipathic

Received: April 16, 2018
Revised: May 15, 2018
Published: May 21, 2018

DOI: 10.1021/acs.langmuir.8b01248
Langmuir 2018, 34, 6777−6783

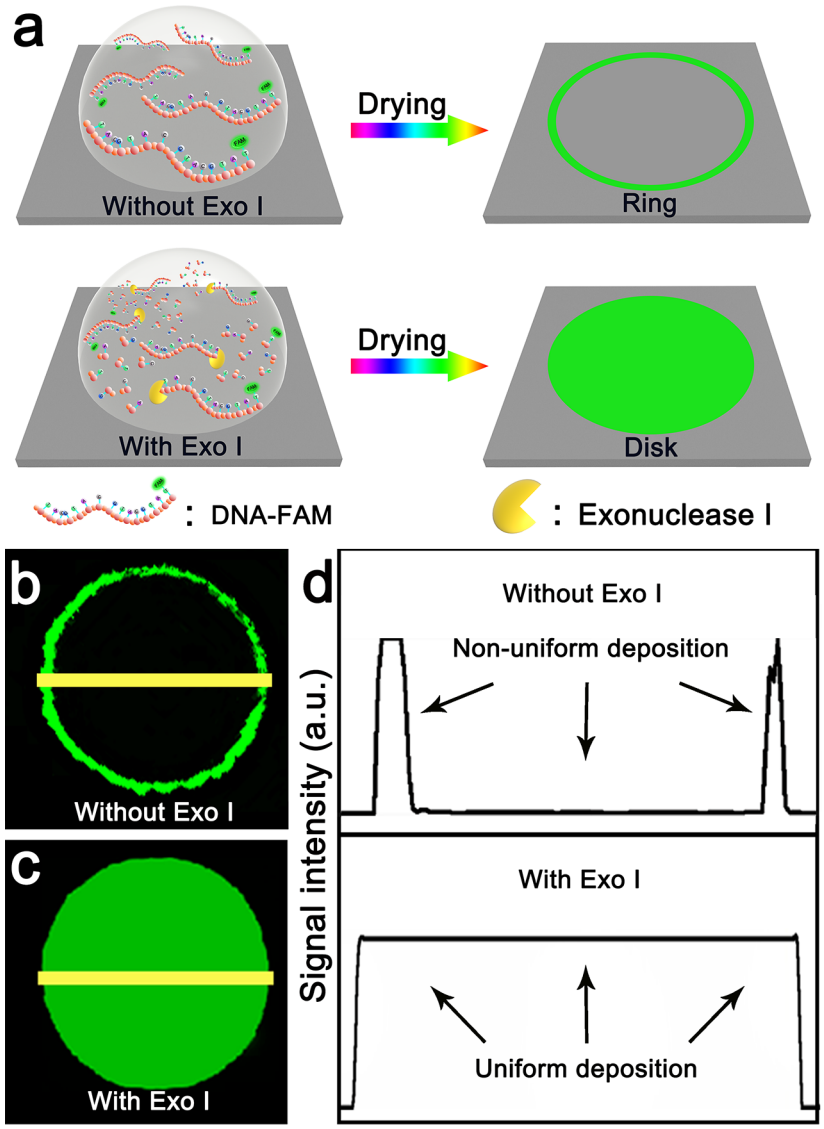

Figure 1. (a) Schematic illustration of eliminating coffee ring effect by nuclease digestion of DNA-FAM. (b) Fluorescent ring left by a sessile drop containing DNA-FAM. (c) Fluorescent disk left by a sessile drop containing DNA-FAM and Exo I. (d) Variation of signal intensity across the fluorescent ring (b) and disk (c) indicated by a solid yellow line.

nucleotide derivatives can efficiently eliminate the coffee ring effect. The mechanism under the elimination of coffee ring effect was further investigated. The results indicated that amphipathic nucleotide derivatives can decrease the surface tension of sessile drops. The decreased surface tension induced the formation of Marangoni flow that can go against the outward capillary flow to reverse the coffee ring effect. Furthermore, surface-assisted sessile drop analysis was designed by integrating the strategy for avoiding coffee ring effect with enzymatic signal amplification. The developed biosensing method displayed a high sensitivity in the detection of target DNA with a minimal detection limit of 1 aM. Discrimination of a single base changes in DNA sequence was also achieved. The surface-assisted sessile drop analysis can open new possibilities for fields such as liquid biopsy and single-nucleotide polymorphisms analysis. Moreover, the strategy for avoiding the coffee ring effect by redefining the amphipathicity of the suspended compounds can further be promoted to other sessile drop systems such as molecular self-assembly, inject printing, and paint manufacturing.[10,37]

RESULTS AND DISCUSSION

Figure 1a illustrates the phenomenon that nuclease digestion of hydrophobic molecules labeled DNA can lead to the formation of a disk instead of a ring on the solid surface after sessile drops have dried. As a proof of concept, random single-stranded DNA molecules (Table S1) labeled with hydrophobic fluorescein amidite (DNA-FAM) were prepared. Exonuclease I (Exo I) that can cut single-stranded DNA to produce nucleotides was used to modify the molecular amphipathicity of DNA-FAM. Without the addition of Exo I, sessile drops containing the DNA-FAM molecules leave a fluorescent ring on the nitrocellulose membrane (Figures S1 and S2) after drying (Figures 1b and S3). The fluorescent rings form because the outward capillary flow inside the sessile drops carry DNA-FAM molecules to the periphery. However, upon digestion of DNA-FAM in the sessile drops by Exo I, uniform fluorescence disks are left on the substrate after evaporation (Figures 1c and S3).

The fluorescence images of the ring (Figure 1b) and disk (Figure 1c) were further converted into grayscale images by the Quantity One Software (Bio-Rad, Version 4.6.9). The variation

DOI: 10.1021/acs.langmuir.8b01248
Langmuir 2018, 34, 6777−6783

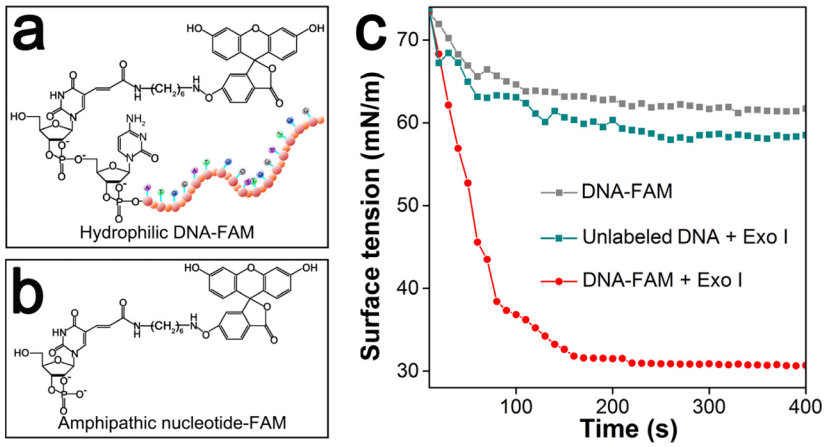

Figure 2. (a) Molecular structures of hydrophilic DNA-FAM and (b) amphipathic nucleotide FAM. (c) Surface tension of the air−water surface vs time for DNA-FAM suspended sessile drops with or without the addition of Exo I.

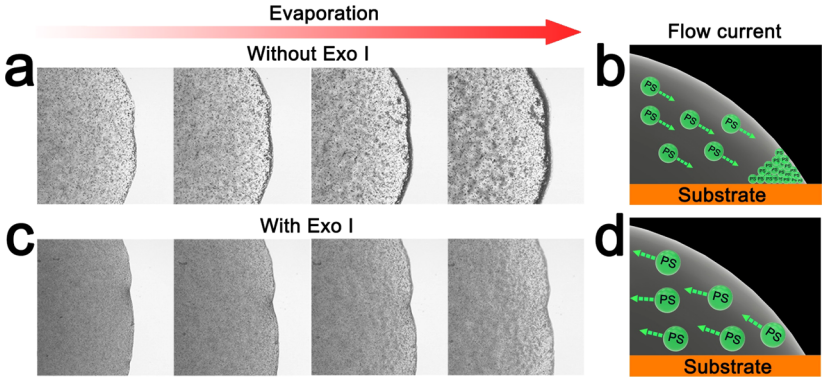

Figure 3. (a) Movement of the PS microspheres in the sessile drops suspended with FAM-DNA. (b) The observed movement of the PS microspheres shown in (a). (c) The movement of the PS microspheres in sessile drops suspended with FAM-DNA and Exo I. (d) The observed movement of the PS microspheres shown in (c).

in gray value across the ring and disk indicated by the solid yellow line is presented in Figure 1d. For the curve indexed to the ring, the signal is predominantly distributed around the contact line and weak signal is also observed in the center region. Moreover, the signal intensity varies on the contact line, suggesting the nonuniform deposition of DNA-FAM in the test zone. In contrast, no obvious variation in signal intensity is observed across the disk, which indicates that the DNA-FAM molecules are uniformly deposited in the test zone. Additionally, DNA labeled with FAM at different sites and DNA labeled with different hydrophobic dyes were treated with Exo I to test the generality of the strategy for eliminating the coffee ring effect. The results showed that all of the digested DNA left fluorescent disk on the substrate after the evaporation of the sessile drops (Figures S4 and S5). The above results clearly demonstrate that nuclease digestion of hydrophobic molecules labeled DNA can efficiently eliminate the coffee ring effect.

The mechanism of reversing the coffee ring effect was further investigated. The difference in molecular structure and physicochemical properties of DNA-FAM and the digested products was studied. The DNA-FAM molecule is hydrophilic due to the presence of a long oligonucleotide chain (Figure 2a). After Exo I digestion, nucleotides and nucleotide-FAM molecules are produced. Sessile drops containing isolated nucleotides and FAM molecules leave fluorescent rings after evaporation (Figure S6), suggesting that the hydrophilic nucleotides cannot lead to the elimination of the coffee ring effect. The nucleotide-FAM molecules were further studied. As shown in Figure 2b, the nucleotide-FAM molecule is amphipathic due to the presence of a comparably weighted hydrophilic nucleotide moiety and a hydrophobic FAM moiety. According to previous studies, amphipathic molecules are able to decrease the surface tension of the sessile drops to induce the Marangoni flow that goes against the outward capillary flow in sessile drops.[38,39] The surface tension of sessile drops containing FAM-DNA, digested unlabeled DNA, and digested FAM-DNA was further measured. As shown in Figure 2c, the FAM-DNA and digested unlabeled DNA led to a slight decrease in the surface tension of the sessile drops. In contrast, the surface tension of the sessile drops containing digested FAM-DNA drastically decreases by about 60%. Accordingly, the amphipathic nucleotide-FAM molecules are suggested to be responsible for the elimination of the coffee ring effect. Other tests further confirm that the nuclease digestion of hydrophobic molecules labeled DNA can serve as a general strategy to eliminate the coffee ring effect (Figures S7−S12).

Previous studies showed that the decrease in the surface tension can induce the formation of an inward Marangoni flow that can recirculate the compounds accumulated at the contact line to the center of the sessile drops.[24,38] The flow currents in sessile drops containing FAM-DNA and digested FAM-DNA were further characterized with video microscopy. Polystyrene (PS) microspheres (Figure S13) are suspended in the sessile drops to aid the observation of the flow currents. The

DOI: 10.1021/acs.langmuir.8b01248
Langmuir 2018, 34, 6777−6783

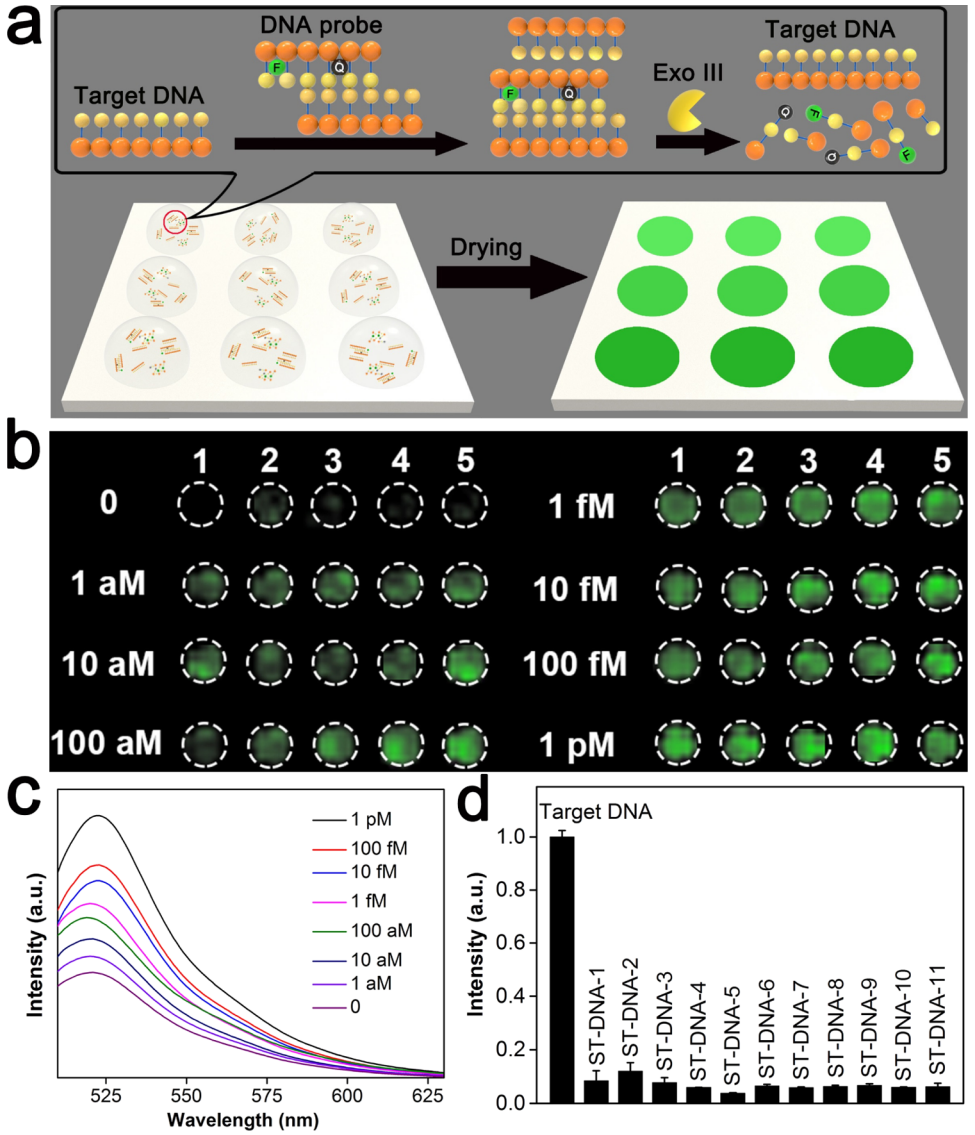

Figure 4. (a) Schematic illustration of the surface-assisted sessile drop analysis. (b) Fluorescent disks left by the biosensing sessile drops containing target DNA with different concentration. (c) Fluorescence spectra of the disks shown in (b). (d) Normalized fluorescence intensities of disks left by biosensing sessile drops added with target DNA and spurious target DNA (ST-DNA).

movement of the PS microspheres over time in the sessile drops was recorded (Videos S1 and S2). In the sessile drops suspended with FAM-DNA and PS microspheres (Figure 3a and Video S1), the microspheres gradually move to the contact line and densely packed microspheres are clearly observed at the periphery as evaporation proceeds. The movement of the PS microspheres in FAM-DNA suspended sessile drops clearly shows the well-known outward capillary flow current that leads to the formation of the ring-shaped structure (Figure 3b). As for the PS microspheres in the sessile drops containing digested FAM-DNA, the inward movement of the PS microspheres toward the center of the drops is clearly observed (Figure 3c and Video S2). The inward flow current (Figure 3d) can be ascribed to the Marangoni flow directed toward the center of the sessile drops.

Taken together, the above results suggest that the nuclease digestion of hydrophilic DNA-FAM to produce an amphipathic nucleotide-FAM in the sessile drops is responsible for the elimination of the coffee ring effect. The amphipathic nucleotide-FAM molecules were carried to the contact line of the sessile drops by an outward capillary flow, making the surface tension around the periphery lower than that in the center region.[40] The surface tension gradient across the sessile drops results in the generation of the Marangoni flow directed toward the center of the drops.[24] Consequently, the nucleotide-FAM and other molecules accumulated around the periphery are carried to the center of the sessile drops by the inward Marangoni flow, finally leading to the formation of a uniform fluorescent disk instead of a ring after drying. These results clearly demonstrate that redefining the amphipathicity of the compounds in sessile drops can serve as an efficient strategy to eliminate the coffee ring effect in the sessile drop systems.

The strategy for avoiding the coffee ring effect was further integrated with enzymatic signal amplification to develop a surface-assisted sessile drop biosensing method. As a proof of concept, DNA was used as the model target. The principle for the visual detection of target DNA on nitrocellulose membrane is illustrated in Figure 4a. Double-stranded toehold exchange probe[41,42] labeled with FAM and hydrophobic quencher BHQ1 was rationally designed (Table S1). The DNA probe has 3′-

DOI: 10.1021/acs.langmuir.8b01248
Langmuir 2018, 34, 6777−6783

protruding terminus to resist cleavage by exonuclease III (Exo III).[43−45] In the presence of target DNA, the DNA probe specifically hybridize with target DNA by toehold-mediated strand displacement[41,42,46] to form probe-target duplex that has a 3′-blunt termini on the probe strand. As Exo III can catalyze the stepwise removal of nucleotides from DNA with the 3′-blunt termini, the probe strand is digested by Exo III and the target DNA is regenerated for the next reaction cycle for signal amplification (Figures S14 and S15). The digestion of the probe strand by Exo III produces amphipathic nucleotide-FAM and nucleotide-BHQ1 molecules (Figure S16) that can induce a Marangoni flow in the sessile drops to drive the formation of uniform fluorescent disks. It should be noted that the Marangoni flow can promote convective mixing of suspended compounds in the sessile drops to increase the collision probability between the reaction molecules to accelerate the reaction. Moreover, the evaporation of the sessile drops can increase the concentration of targets through volume reduction, which is particularly suitable for the analysis targets with low abundance (Figure S17).

Figure 4b presents the fluorescent images left by the biosensing sessile drops containing different concentrations of target DNA after drying. Notably, the coffee ring effect is efficiently avoided and uniform fluorescence disks are formed (Figure S18), which can be ascribed to the production of amphipathic molecules by Exo III digestion. The fluorescence intensity of the disks gradually increases with raising the amounts of added target DNA (Figures 4b and S19). Moreover, sessile drops containing 1 aM of target DNA leaves legible disks on the nitrocellulose membrane with bright fluorescence, suggesting that the surface-assisted sessile drop analysis possesses high sensitivity in target DNA detection. The fluorescence spectra of the disks are presented in Figure 4c. The emission peak indexed to FAM grows stronger with increasing concentration of target DNA and obvious signal enhancement is observed with adding 1 aM of target DNA. The high sensitivity of the surface-assisted sessile drop analysis can be ascribed to the collective enzymatic signal amplification and evaporation-induced concentration of targets. The specificity of the surface-assisted sessile drop analysis for target DNA detection was further investigated by evaluating the response of the biosensing sessile drops to spurious target DNA (ST-DNA) that only have a single-base difference with the target DNA (Table S1). As shown in Figure 4d, all of the spurious targets lead to a slight increase in the fluorescence intensity compared to the target DNA, suggesting that the toehold exchange probe is able to discriminate single-base changes in DNA sequence. The above results clearly demonstrated that highly sensitive and specific surface-assisted sessile drop analysis has been successfully developed based on the strategy for reversing the coffee ring effect.

CONCLUSIONS

In this work, we found that the nuclease digestion of hydrophobic molecules labeled DNA in sessile drops can efficiently eliminate the coffee ring effect. Amphipathic molecules produced in the nuclease digestion can induce a Marangoni flow in the sessile drops to drive the formation of a disk-like structure instead of a ring-shaped structure after drying. Surface-assisted sessile drop analysis was further developed by combining the strategy of eliminating the coffee ring effect with enzymatic signal amplification. The developed biosensing method possesses high sensitivity and specificity. The surface-assisted sessile drop analysis can open new possibilities for single nucleotide polymorphisms analysis and liquid biopsy. Also, the developed strategy for avoiding coffee ring effect by redefining the amphipathicity of suspended compounds can further be promoted to other sessile drop systems including molecular self-assembly and paint manufacturing.

EXPERIMENTAL SECTION

Printing Hydrophobic Polydimethylsiloxane (PDMS) Circles on Nitrocellulose Membrane. Hydrophobic PDMS circles (diameter of ∼2.5 mm) were printed onto a nitrocellulose membrane with a three-dimensional (3D) printer. The mechanical arm of the 3D printer moved an injector over the nitrocellulose membrane to print the PDMS circle and the nitrocellulose membrane was moved by a separate motor along the axis perpendicular to the motion of the mechanical arm. The resultant nitrocellulose membrane was heated at 90 °C in an electric oven for 6 min to allow PDMS to fully penetrate the nitrocellulose membrane. The as-prepared PDMS layer can trap the sessile drops within the circles.

Elimination of Coffee Ring Effect with Nuclease Digestion of DNA-FAM. In a typical experiment, 10 μL of 1× NEB buffer 1 (10 mM Bis-Tris-propane HCl, pH 7.0, 10 mM $MgCl_2$, 1 mM dithiothreitol) containing DNA-FAM (200 nM) and Exo I (40 U) was spotted to the hydrophobic PDMS circles on the nitrocellulose membrane to form a sessile drop. The sessile drop was kept at 37 °C until dry. The fluorescent images were captured with a fluorescence & FISH digital pathology scanner (Aperio VERSA 8, Leica) equipped with a 488 nm laser. The control experiments were conducted using the same procedure in the absence of Exo I.

Measurement of Surface Tension. Briefly, 50 μL of 1× NEB buffer 1 suspended with DNA-FAM (200 nM) and Exo I (40 U) was allowed to react at 37 °C for 2 h with humidity control. The dynamic surface tension measurement was then conducted by the hanging droplet method on a KRUSS Drop Shape Analysis (DSA-10). The surface tension of the sessile drops was determined by comparing the shape of the drop hanging from a syringe to the Young−Laplace equation. The capillary tip of the outside diameter was 0.76 mm. The dynamic surface tension was measured with a custom-built improvement to the pendant drop system. Evaporation was suppressed by sealing the reaction drops in a cuvette with an excess of solvent. No obvious evaporation was observed during the experiments. Each dynamic surface tension measurement was repeated three times. Control experiments without the addition of Exo I were carried out with the same procedure.

Observation of Marangoni Flow in Sessile Drops. Typically, the reaction mixture containing 1× NEB buffer 1, 400 U Exo I, and 200 nM DNA-FAM was prepared and allowed to react at 37 °C for 2 h. Then, the PS microspheres (0.3%) were added to the above reaction solution. The mixture was further dropped on thin glass coverslips for microscopic observation. The bright field images and videos about the movements of PS microspheres in the sessile drops were obtained on a Zeiss confocal laser scanning microscope (LSM 880).

Elimination of Coffee Ring Effect in Surface-Assisted Sessile Drop Analysis. A volume of 10 μL reaction mixture containing 1× NEB buffer 1, Exo III (40 U), toehold exchange probe (200 nM), and target DNA (0.1 nM) was spotted to the test zone on a nitrocellulose membrane. The reaction in the sessile drops was allowed to proceed at 37 °C for 2 h. The fluorescent images were captured using the fluorescence & FISH digital pathology scanner (Aperio VERSA 8, Leica).

Detection of Target DNA with the Surface-Assisted Sessile Drop Analysis. In a typical experiment, a series of reaction solution containing 1× NEB buffer 1, 40 U Exo III, 200 nM toehold exchange probe, and different concentrations of target DNA (0−1 pM) were prepared. Then, 10 μL of the reaction solutions was spotted to the test zones on the nitrocellulose membrane and was allowed to react at 37 °C for 2 h. The fluorescence intensity of the left disks were quantified on the IVIS Spectrum (PerkinElmer). The fluorescence spectra of the

DOI: 10.1021/acs.langmuir.8b01248
Langmuir 2018, 34, 6777−6783

disks were recorded by a fluorescence microplate reader with excitation wavelengths of 488 nm.

■ ASSOCIATED CONTENT

Supporting Information

The Supporting Information is available free of charge on the ACS Publications website at DOI: 10.1021/acs.langmuir.8b01248.

Chemicals, instruments, experimental details, DNA sequences, fluorescent images left by sessile drops containing different kinds of DNA treated with nuclease, principles of enzymatic signal amplification, molecular structure of the amphipathic nucleotide-BHQ1 molecule (PDF)

Sessile drops suspended with FAM-DNA and PS microspheres (AVI)

PS microspheres in the sessile drops containing digested FAM-DNA, the inward movement of the PS microspheres toward the center of the drops (AVI)

■ AUTHOR INFORMATION

Corresponding Author

*E-mail: yuanquan@whu.edu.cn.

ORCID

Jie Wang: 0000-0003-4170-8470

Quan Yuan: 0000-0002-3085-431X

Author Contributions

‖C.H. and J.W. contributed equally to this work.

Author Contributions

The manuscript was written through contributions of all the authors. All the authors have given approval to the final version of the manuscript.

Notes

The authors declare no competing financial interest.

■ ACKNOWLEDGMENTS

This work was supported by the National Key R&D Program of China (2017YFA0208000), the National Natural Science Foundation of China (21675120), National Basic Research Program of China (973 Program, Grants 2015CB932600), Ten Thousand Talents Program for Young Talents, and the start-up Research Fund for Prof. Q.Y. (531107050973, 531109010053), State Key Laboratory of Chemo/Biosensing and Chemometrics at Hunan University (734106172). We sincerely thank Prof. Chad A. Mirkin at Northwestern University for critical reading of the manuscript.

■ REFERENCES

(1) Deegan, R. D.; Bakajin, O.; Dupont, T. F.; Huber, G.; Nagel, S. R.; Witten, T. A. Capillary Flow as the Cause of Ring Stains from Dried Liquid Drops. *Nature* **1997**, *389*, 825−827.

(2) Yunker, P. J.; Still, T.; Lohr, M. A.; Yodh, A. Suppression of the Coffee-Ring Effect by Shape-Dependent Capillary Interactions. *Nature* **2011**, *476*, 308−311.

(3) Kuang, M.; Wang, L. B.; Song, Y. L. *Adv. Mater.* **2014**, *26*, 6950−6958.

(4) Anyfantakis, M.; Baigl, D. Manipulating the Coffee-Ring Effect: Interactions at Work. *ChemPhysChem* **2015**, *16*, 2726−2734.

(5) Li, Y. N.; Yang, Q.; Li, M. Z.; Song, Y. L. *Sci. Rep.* **2016**, *6*, No. 24628.

(6) Hu, H.; Larson, R. G. Evaporation of a Sessile Droplet on a Substrate. *J. Phys. Chem. B* **2002**, *106*, 1334−1344.

(7) Cai, Y.; Zhang, B. M. N. Marangoni Flow-Induced Self-Assembly of Hexagonal and Stripelike Nanoparticle Patterns. *J. Am. Chem. Soc.* **2008**, *130*, 6076−6077.

(8) Sun, J. Z.; Bao, B.; He, M.; Zhou, H. H.; Song, Y. L. *ACS Appl. Mater. Interfaces* **2015**, *7*, 28086−28099.

(9) Devineau, S.; Anyfantakis, M.; Marichal, L.; Kiger, L.; Morel, M.; Rudiuk, S.; Baigl, D. Protein Adsorption and Reorganization on Nanoparticles Probed by the Coffee-Ring Effect: Application to Single Point Mutation Detection. *J. Am. Chem. Soc.* **2016**, *138*, 11623−11632.

(10) Dugyala, V. R.; Basavaraj, M. G. Evaporation of Sessile Drops Containing Colloidal Rods: Coffee-Ring and Order-Disorder Transition. *J. Phys. Chem. B* **2015**, *119*, 3860−3867.

(11) Trantum, J. R.; Wright, D. W.; Haselton, F. R. Biomarker-Mediated Disruption of Coffee-Ring Formation as a Low Resource Diagnostic Indicator. *Langmuir* **2011**, *28*, 2187−2193.

(12) Hou, J.; Zhang, H. C.; Su, B.; Li, M. Z.; Yang, Q.; Jiang, L.; Song, Y. L. *Chem. - Asian J.* **2016**, *11*, 2680−2685.

(13) Shen, W.; Li, M.; Ye, C.; Jiang, L.; Song, Y. Direct-Writing Colloidal Photonic Crystal Microfluidic Chips by Inkjet Printing for Label-Free Protein Detection. *Lab Chip* **2012**, *12*, 3089−3095.

(14) Hernandez-Perez, R.; Fan, Z. H.; Garcia-Cordero, J. L. Evaporation-Driven Bioassays in Suspended Droplets. *Anal. Chem.* **2016**, *88*, 7312−7317.

(15) Ding, Y.; Ling, J.; Qiao, Y.; Li, Z.; Sun, Z.; Cai, J.; Guo, Y.; Wang, H. A High-Throughput Fluorimetric Microarray with Enhanced Fluorescence and Suppressed "Coffee-Ring" Effects for the Detection of Calcium Ions in Blood. *Sci. Rep.* **2016**, *6*, No. 38602.

(16) Chen, T. H.; Yu, C. J.; Tseng, W. L. Sinapinic Acid-Directed Synthesis of Gold Nanoclusters and Their Application to Quantitative Matrix-Assisted Laser Desorption/Ionization Mass Spectrometry. *Nanoscale* **2014**, *6*, 1347−1353.

(17) Park, J.; Moon, J. Control of Colloidal Particle Deposit Patterns within Picoliter Droplets Ejected by Ink-Jet Printing. *Langmuir* **2006**, *22*, 3506−3513.

(18) Lin, C. C.; Yang, Y. M.; Liao, P. H.; Chen, D. W.; Lin, H. P.; Chang, H. C. A Filter-Like Aunps@MS SERS Substrate for *Staphylococcus aureus* Detection. *Biosens. Bioelectron.* **2014**, *53*, 519−527.

(19) Wang, H.; Fang, J.; Xu, J.; Wang, F.; Sun, B.; He, S.; Sun, G.; Liu, H. A Hanging Plasmonic Droplet: Three-Dimensional SERS Hotspots for a Highly Sensitive Multiplex Detection of Amino Acids. *Analyst* **2015**, *140*, 2973−2978.

(20) Rao, A. N.; Vandencasteele, N.; Gamble, L. J.; Grainger, D. W. High-Resolution Epifluorescence and Time-of-Flight Secondary Ion Mass Spectrometry Chemical Imaging Comparisons of Single DNA Microarray Spots. *Anal. Chem.* **2012**, *84*, 10628−10636.

(21) Coppé, J. P.; Xu, Z.; Chen, Y.; Liu, G. L. Metallic Nanocone Array Photonic Substrate for High-Uniformity Surface Deposition and Optical Detection of Small Molecules. *Nanotechnology* **2011**, *22*, No. 245710.

(22) Sola, L.; Damin, F.; Cretich, M.; Chiari, M. Novel Polymeric Coatings with Tailored Hydrophobicity to Control Spot Size and Morphology in DNA Microarray. *Sens. Actuators, B* **2016**, *231*, 412−422.

(23) Anyfantakis, M.; Baigl, D. Dynamic Photocontrol of the Coffee-Ring Effect with Optically Tunable Particle Stickiness. *Angew. Chem., Int. Ed.* **2014**, *53*, 14077−14081.

(24) Sempels, W.; De Dier, R.; Mizuno, H.; Hofkens, J.; Vermant, J. Auto-Production of Biosurfactants Reverses the Coffee Ring Effect in a Bacterial System. *Nat. Commun.* **2013**, *4*, No. 1757.

(25) Dong, Y.; Yang, Y. R.; Zhang, Y.; Wang, D.; Wei, X.; Banerjee, S.; Liu, Y.; Yang, Z.; Yan, H.; Liu, D. Cuboid Vesicles Formed by Frame-Guided Assembly on DNA Origami Scaffolds. *Angew. Chem., Int. Ed.* **2017**, *56*, 1586−1589.

(26) Zhou, W.; Saran, R.; Liu, J. Metal Sensing by DNA. *Chem. Rev.* **2017**, *117*, 8272−8325.

(27) Dong, Y.; Yang, Z.; Liu, D. DNA Nanotechnology Based on i-Motif Structures. *Acc. Chem. Res.* **2014**, *47*, 1853−1860.

DOI: 10.1021/acs.langmuir.8b01248
Langmuir 2018, 34, 6777−6783

(28) Wang, F.; Liu, Z.; Wang, B.; Feng, L.; Liu, L.; Lv, F.; Wang, Y.; Wang, S. Multi-Colored Fibers by Self-Assembly of DNA, Histone Proteins, and Cationic Conjugated Polymers. *Angew. Chem., Int. Ed.* **2014**, *53*, 424−428.
(29) Jiang, Y.; Zhu, C. F.; Ling, L. S.; Wan, L. J.; Fang, X. H.; Bai, C. L. Specific Aptamer-Protein Interaction Studied by Atomic Force Microscopy. *Anal. Chem.* **2003**, *75*, 2112−2116.
(30) Wang, R.; Jin, C.; Zhu, X.; Zhou, L.; Xuan, W.; Liu, Y.; Liu, Q.; Tan, W. Artificial Base zT as Functional "Element" for Constructing Photoresponsive DNA Nanomolecules. *J. Am. Chem. Soc.* **2017**, *139*, 9104−9107.
(31) Jia, Y.; Gao, P.; Zhuang, Y.; Miao, M.; Lou, X.; Xia, F. Facile Probe Design: Fluorescent Amphiphilic Nucleic Acid Probes without Quencher Providing Telomerase Activity Imaging Inside Living Cells. *Anal. Chem.* **2016**, *88*, 6621−6626.
(32) Pei, H.; Zuo, X.; Zhu, D.; Huang, Q.; Fan, C. Functional DNA Nanostructures for Theranostic Applications. *Acc. Chem. Res.* **2013**, *47*, 550−559.
(33) Li, F.; Zhang, H. Q.; Wang, Z. X.; Newbigging, A. M.; Reid, M. S.; Li, X. F.; Le, X. C. Aptamers Facilitating Amplified Detection of Biomolecules. *Anal. Chem.* **2015**, *87*, 274−292.
(34) Torabi, S. F.; Wu, P.; McGhee, C. E.; Chen, L.; Hwang, K.; Zheng, N.; Cheng, J.; Lu, Y. In Vitro Selection of a Sodium-Specific Dnazyme and Its Application in Intracellular Sensing. *Proc. Natl. Acad. Sci. U.S.A.* **2015**, *112*, 5903−5908.
(35) Wang, Y.; Wu, C. C.; Chen, T.; Sun, H.; Cansiz, S.; Zhang, L. Q.; Cui, C.; Hou, W. J.; Wu, Y.; Wan, S.; Cai, R.; Liu, Y.; Sumerlin, B. S.; Zhang, X. B.; Tan, W. H. DNA Micelle Flares: a Study of the Basic Properties That Contribute to Enhanced Stability and Binding Affinity in Complex Biological Systems. *Chem. Sci.* **2016**, *7*, 6041−6049.
(36) Jin, C.; Liu, X. J.; Bai, H. R.; Wang, R. W.; Tan, J.; Peng, X. H.; Tan, W. H. Engineering Stability-Tunable DNA Micelles Using Photocontrollable Dissociation of an Intermolecular G-Quadruplex. *ACS Nano* **2017**, *11*, 12087−12093.
(37) Benson, J.; Fung, C. M.; Lloyd, J. S.; Deganello, D.; Smith, N. A.; Teng, K. S. Direct Patterning of Gold Nanoparticles Using Flexographic Printing for Biosensing Applications. *Nanoscale Res. Lett.* **2015**, *10*, No. 127.
(38) Trantum, J. R.; Baglia, M. L.; Eagleton, Z. E.; Mernaugh, R. L.; Haselton, F. R. Biosensor Design Based on Marangoni Flow in an Evaporating Drop. *Lab Chip* **2014**, *14*, 315−324.
(39) Garcia-Cordero, J. L.; Fan, Z. H. Sessile Droplets for Chemical and Biological Assays. *Lab Chip* **2017**, *17*, 2150−2166.
(40) Kajiya, T.; Kobayashi, W.; Okuzono, T.; Doi, M. Controlling the Drying and Film Formation Processes of Polymer Solution Droplets with Addition of Small Amount of Surfactants. *J. Phys. Chem. B* **2009**, *113*, 15460−15466.
(41) Zhang, D. Y.; Chen, S. X.; Yin, P. Optimizing the Specificity of Nucleic Acid Hybridization. *Nat. Chem.* **2012**, *4*, 208−214.
(42) Xu, H.; Deng, W.; Huang, F.; Xiao, S.; Liu, G.; Liang, H. Enhanced DNA Toehold Exchange Reaction on a Chip Surface to Discriminate Single-Base Changes. *Chem. Commun.* **2014**, *50*, 14171−14174.
(43) Qu, X.; Zhu, D.; Yao, G.; Su, S.; Chao, J.; Liu, H.; Zuo, X.; Wang, L.; Shi, J.; Wang, L.; et al. An Exonuclease III-Powered, On-Particle Stochastic DNA Walker. *Angew. Chem., Int. Ed.* **2017**, *56*, 1855−1858.
(44) Duan, R.; Zuo, X.; Wang, S.; Quan, X.; Chen, D.; Chen, Z.; Jiang, L.; Fan, C.; Xia, F. Lab in a Tube: Ultrasensitive Detection of MicroRNAs at the Single-Cell Level and in Breast Cancer Patients Using Quadratic Isothermal Amplification. *J. Am. Chem. Soc.* **2013**, *135*, 4604−4607.
(45) Zuo, X.; Xia, F.; Xiao, Y.; Plaxco, K. W. Sensitive and Selective Amplified Fluorescence DNA Detection Based on Exonuclease III-Aided Target Recycling. *J. Am. Chem. Soc.* **2010**, *132*, 1816−1818.
(46) You, M.; Lyu, Y.; Han, D.; Qiu, L.; Liu, Q.; Chen, T.; Wu, C. S.; Peng, L.; Zhang, L.; Bao, G.; et al. DNA Probes for Monitoring Dynamic and Transient Molecular Encounters on Live Cell Membranes. *Nat. Nanotechnol.* **2017**, *12*, 453−459.

DOI: 10.1021/acs.langmuir.8b01248
Langmuir 2018, 34, 6777−6783